

Comparing Models of Subject-Clustered Single-Cell Data

Lee Panter

Audrey Hendricks, PhD-Committee Chair and Advisor*

Stephanie Santorico, PhD-Committee Member*

Rhonda Bacher†, PhD-Committee Member

Abstract

Single-Cell RNA sequencing data represents a revolutionary shift to approaches being used to decode the human transcriptome. Such data are becoming more prevalent and are gathered on ever-larger samples of individuals, enabling analysis of subject level relationships. However, it is not always clear how to conduct this subject level analysis. Current methods often do not account for nested study designs in which samples of hundreds, or thousands of cells are gathered from multiple individuals. Therefore, there is a need to outline, analyze, and compare methods for estimating subject level relationships in single-cell RNA sequencing expression.

Here, I compare five modeling strategies for detecting subject level associations using single-cell RNA sequencing expression: linear regression, linear regression with subjects modeled as fixed effects, linear mixed effects models with subjects modeled as random intercepts only or both random intercepts and random slopes, and generalized estimating equations. I first present each method. I then compare the regression estimates and standard errors for each method using real single-cell data from a Lupus Nephritis study of 27 subjects. I hope that this paper presents insights into methods to analyze subject level associations from single-cell expression data.

*The University of Colorado-Denver

†The University of Florida

Introduction

Traditional methods of sequencing the human transcriptome involve analyzing the combined genetic material of thousands or even millions of cells. These so called “bulk” techniques provide information about the average gene expression across the cell sample but often fail to capture the underlying variability in expression profiles within the sample of cells [1].

Conversely, single-cell RNA sequencing (scRNA-seq) obtains measurements of transcriptomic information specific to individual cells. Hundreds or even thousands of RNA-sequencing profile measurements, each specific to a single-cell, can be used to estimate expression variability across the cells within the sample. This feature of single-cell data analysis is suited for research applications that seek to identify rare cellular subpopulations or characterize expressions that are differentially expressed across conditions [2]. Additionally, technological developments have made generating single-cell data more cost effective, and easier to obtain on multiple sample-sources, most notably on multiple individuals.

The utility of single-cell data, and the feasibility of single-cell data measurements across multiple subjects motivates a need to compare methods that can adequately model single-cell data while accounting for the correlation of repeated measures within subjects (many single-cell observations within each subject).

Here, I compare five methods for modeling scRNA-seq expression profiles that account for within-subject correlation: linear modeling (LM), linear modeling with subjects as fixed effects (LM-FE), linear mixed effects models with subjects only as random intercepts (LMM-RI) or as both random intercepts and random slopes (LMM-RS), and generalized estimating equations (GEE). I first present the overall framework for each method. Then I compare the results for each model using single-cell data from a study of 27 Lupus Nephritis cases.

Description of Data Set

Throughout this paper references are made to the 2018 article entitled “The immune cell landscape in kidneys with lupus nephritis patients”, in which Arazi, Rao, Berthier, et al. compare single-cell kidney tissue sample data from 45 Lupus Nephritis subjects vs. 25 population controls [3]. The kidney tissue samples were collected from ten clinical sites across the United States, cryogenically frozen, then shipped to a central processing facility. At the central processing facility, the tissue samples were then thawed, and sorted into single-cell suspension across 384-well plates using FlowJo 10.0.7, 11-color flow cytometry [4]. Single-cell RNA sequencing was performed using a modified CEL-Seq2 method [5] with ~ 1 million paired-end reads per cell. The original experimental data may be accessed by visiting the Immport repository with accession code SDY997. Immport-SDY997: <https://www.immport.org/shared/study/SDY997>

The original research conducted in Arazi, Rao, Berthier, et al, concerned 70 subjects. A subset of 9,560 single-cell observations originating from 27 subjects of the original data is used in the analysis I conduct for this study. Markers of case/control status for each subject are not present. However, for each single-cell observation there are:

- More than $3.8 * 10^4$ RNA sequencing measurements
- 23 Flow Cytometry measurements
- 10 meta data-variables (e.g. subject of origin, and cell type)

I implement a substantial quality control (QC) process to filter observations that are inadequately representative of living, single-cell, samples from an agglomerated case/control population (with cases of Lupus Nephritis). Inadequate (poor/low quality) observations are filtered out if they are either: not a single-cell (multiple or missing cells), or cellular material that is insufficiently alive . Details related to the QC filtering process are contained in Appendix A-Data Quality Control. After QC, 1110 observations originating from 15 subjects

remain for analysis.

I focus on two pairs of RNA sequencing variables for model comparisons. I use the two outcome variables: *MALAT1* and *FBLN1* due to previously established associations with human disease conditions [6] [7]. I calculate pairwise correlations for each of the outcome variables. I choose the Cluster of Differentiation marker with the highest correlation to pair as a predictor to each of the outcome variables. I perform a log-transformation on the predictor and response of both variable pairings motivated by each variable’s right-skewed distribution.

I will use the following transformed variable pairings to perform model comparisons:

1. $MALAT1 \sim CD19 \quad \mapsto \quad \log(MALAT1) \sim \log(CD19)$
2. $FBLN1 \sim CD34 \quad \mapsto \quad \log(FBLN1) \sim \log(CD34)$

Further details related to variable selection and summaries are contained in Appendix B-Variable Selections and Summaries.

Model Descriptions

In the following sections a description is provided for each model using the following notation for a subject level response and predictor pair:

$$(X_{ij}, Y_{ij}) \quad \text{for } i = 1, \dots, N \quad j = 1, \dots, n_i$$

where $i = 1, \dots, N$ represents the observation’s *subject of origination* (subject from which the measurement was taken), and $j = 1, \dots, n_i$ represents the measurement index taken within subject i (the repeated measure index within each subject).

Linear Model (LM)

The linear model can be written as:

$$Y_{ij} = \beta_0 + \beta_1 X_{ij} + \epsilon_{ij}$$

This model does not account for correlation structure in the data, and instead assumes the observations are independent. Linear model parameter estimates are for the population averages.

The error term, ϵ_{ij} , is assumed to be a normally distributed random variable with mean zero and variance σ_ϵ^2 .

Linear Model with Fixed-Effect (LM-FE)

Adding a subject-specific intercept term to the LM model allows for the accounting of subject level effects by uniformly shifting the mean of the fitted values specific to a subject. This model is written as:

$$Y_{ij} = \beta_0 + \beta_{1i}(\text{subject}_j) + \beta_2 X_{ij} + \epsilon_{ij}$$

where

$$\beta_i(\text{subject}_j) = \begin{cases} \beta_i & \text{if } i = j \\ 0 & \text{if } i \neq j \end{cases} \quad \text{for } i = 2, \dots, N$$

This model adds $N - 1$ estimated parameters $\hat{\beta}_{1i}$ which represent the average deviation for each subject from the global estimated mean Linear Model (LM).

Linear Mixed Effects Models

Linear mixed effects models that incorporate subjects using random effects are the next methods outlined. Linear mixed effects models do not require the assumption of independent observations. Structures such as autoregressive, moving-average, or simply unrestricted (unstructured) can be used to explicitly model within-subject correlation. Additionally, random effects can be incorporated and fit with covariance parameters that capture between-subject effects.

Linear Mixed Effects Model with Random Intercept (LMM-RI)

A linear mixed effects model with a random intercept controls for subject-level correlations through the use of subject-specific variances. The LMM-RI model is written as:

$$Y_{ij} = \beta_0 + \beta_1 X_{ij} + b_{0i}(\text{subject}_i) + \epsilon_{ij}$$

where

$$b_{0i} \sim N(0, \sigma_b^2) \quad \epsilon_{ij} \sim N(0, \sigma_\epsilon^2)$$

$$\text{for } i \in \{1, \dots, N\} \quad \text{and} \quad j \in \{1, \dots, n_i\}$$

it is assumed that b_{0i} and ϵ_{ij} are independent.

Linear Mixed Effect Model with Random Slope (LMM-RS)

A random slope linear mixed effects model differs from each of the previously considered methods because it allows for distinct relationships for each subject between the predictor and response variables of interest. The LMM-RS model is written as:

$$Y_{ij} = \beta_0 + \beta_1 X_{ij} + b_{0i}(\text{subject}_i) + [b_{1i}(\text{subject}_i) X_{ij}] + \epsilon_{ij}$$

where

$$\mathbf{b} = \begin{bmatrix} b_{0i} \\ b_{1i} \end{bmatrix} \sim N(\mathbf{0}, \mathbf{G})$$

$$G = \begin{bmatrix} \sigma_{b_0}^2 & \sigma_{b_{01}} \\ \sigma_{b_{10}} & \sigma_{b_1}^2 \end{bmatrix}$$

$$\epsilon_{ij} \sim N(\mathbf{0}, \sigma_\epsilon^2 \mathbf{I}_{n_i})$$

Generalized Estimating Equations (GEE)

The final modeling method considered is generalized estimating equations (GEE). The GEE framework requires the specification of a systematic, and random component. It also requires the specification of an assumed covariance structure. This structure specifies the within-subject correlation, for which the GEE algorithm iteratively refits estimated values.

The components for the GEE model are:

- The random component
 - It is assumed the responses are *approximately* normally distributed.
- The systematic component
 - It is assumed that the linear predictor η_{ij} is a linear combination of the covariates

$$\eta_{ij} = \beta_0 + \beta_1 X_{ij}$$

- The link function
 - It is assumed that the link function $g(\mu_{ij}) = \mu_{ij}$ provides the relationship between the linear predictor and the expected outcome, i.e:

$$E[Y_{ij}|X_{ij}] = g(\mu_{ij}) = \mu_{ij} = \eta_{ij} = \beta_0 + \beta_1 X_{ij}$$

- Working Covariance Structure
 - It is assumed that observations within a subject are independent, therefore:

$$[Cov(Y_{ij}, Y_{ik})]_{jk} = \begin{cases} Var(Y_{ij}) & \text{if } j = k \\ 0 & \text{if } j \neq k \end{cases}$$

$$for \quad j, k \in \{1, \dots, n_i\}$$

Estimates for GEE parameters are calculated by solving an *estimating equation* using the Newton-Raphson iterative root-finding algorithm. Detailed method descriptions, including derivation and solving of the estimating equations can be found in Fitzmaurice, Laird, and Ware [8].

The GEE algorithm is robust to misspecification of the working covariance structure. So initially incorrect specifications of the working covariance matrix still converge to the appropriate structure form with algorithmic iteration. This stability is due in-part to the fact that the method estimates population-average effects.

Parameter Interpretations

Excepting the LM-FE and the LMM-RS models, each of the modeling methods previously described are techniques used for obtaining estimates of population-averaged parameters. These parameter values are interpreted as contributing to the response of the average subject

(not representative of any single subject within the sample).

An interpretation of this parameter is: **across all subjects, a one-unit increase in the predictor (X_{ij}) is associated with a $(\hat{\beta})$ unit change in the expected outcome (Y_{ij})**

Conversely, the LMM-RS modeling method is a technique used for obtaining estimates of subject-specific parameters. These parameter values are interpreted as contributing to the average response having conditioned on a specific subject within the data.

An interpretation of this parameter is: **after having conditioned on a specific subject a one-unit increase in the predictor (X_{ij}) is associated with a $(\hat{\beta})$ unit change in the expected outcome (Y_{ij}).**

Finally, the LM-FE method is a technique used for obtaining estimates of population-averaged parameters adjusting for average subject effect. These parameters are interpreted as contributing to the response of the average subject after adjusting for a each subject's average effect.

An interpretation of this parameter is: **across all subjects, after having adjusted for the effect of each subject's average effect, a one-unit increase in the predictor (X_{ij}) is associated with a $(\hat{\beta})$ unit change in the expected outcome (Y_{ij}).**

Results

Parameter Value Comparisons

A comparison of main effect slope coefficient, standard error and test statistic (shown in **Tables (3) - (4)** below) across modeling approaches within variable pairings indicates that estimates produced by the LM and GEE methods are similar down to 10^{-4} . The LM-FE and LMM-RI method estimates are also similar since estimates for each parameter type

(coefficient, standard error and test statistic) exhibit magnitude and directional similarities in both variable pairings.

The LMM-RS estimates for the fixed effect slope parameter standard error is the largest when compared to the corresponding estimates within variable pairing as generated by other modeling methods. In contrast, the standard error of the fixed effect slope parameter is smallest for the LMM-RI model within variable pairings. The LM-FE model has a smaller fixed effect slope standard error than either the LM or the GEE model within both variable combinations.

The differences in test statistics of the fixed effect slope parameter for each modeling method within each variable pairing are analogous to the differences in slope coefficients previously noted. In particular, test statistics have similar values between the LM and GEE models as well as between the LM-FE and LMM-RI models. Test statistics calculated for the LMM-RS model are the least similar to the other modeling methods. The LMM-RS model averages test statistics that are 86% larger than the other models. This decreased similarity is also accompanied by decreased parameter significance.

Model Designation	Model Description	Estimate	Std. Error	Test Statistic	p-value
LM	Linear Model	4.918e-2	1.455e-2	3.381	7.47e-4
LM-FE	Linear Model with Fixed-Effect Intercept	4.833e-2	1.381e-2	3.500	4.84e-4
LMM-RI	Linear Mixed Model with Random Intercept	4.920e-2	1.374e-2	3.579	3.6e-4
LMM-RS	Linear Mixed Model with Random Slope	5.938e-2	3.538e-2	1.678	1.19e-1
GEE	Generalized Estimating Equations	4.918e-2	1.455e-2	3.381**	7.47e-4

Table 3. $MALAT1 \sim CD19$ model estimates: Fixed effect slope estimate, standard error, test statistic, and p-value for each model for the relationship between the predictor $CD19$ and the

outcome *MALAT1*. ** Approximate Wald-Z distribution.

Model Designation	Model Description	Estimate	Std. Error	Test Statistic	p-value
LM	Linear Model	7.884e-1	4.92e-2	4.002	<2e-16
LM-FE	Linear Model with Fixed-Effect Intercept	1.31e-1	3.42e-2	3.818	1.42e-4
LMM-RI	Linear Mixed Model with Random Intercept	1.35e-1	3.42e-2	3.95	8.4e-5
LMM-RS	Linear Mixed Model with Random Slope	1.705e-1	7.29e-2	2.34	6.7e-2
GEE	Generalized Estimating Equations	7.884e-1	4.92e-2	4.002**	< 2e-16

Table 4. *FBLN1* ~ *CD34* model estimates: Fixed effect slope estimate, standard error, test statistic, and p-value for each model for the relationship between the predictor *CD34* and the outcome *FBLN1*. ** Approximate Wald-Z distribution.

Displayed in **tables (5) - (10)** below are percent change in: parameter estimate, standard error, and test statistic for the *MALAT1* ~ *CD19* variable pairing in **tables (5)-(7)** and the *FBLN1* ~ *CD34* variable paring in **tables (8)-(10)**. Where the percent change in estimate is defined as:

$$\text{Percent Change } [A]_{ij} = \left(\frac{A_j - A_i}{A_i} \right) * 100$$

Model	LM	LM-FE	LMM-RI	LMM-RS	GEE
LM	0	-1.7283	0.0407	20.7401	0.0000
LM-FE	1.7587	0	1.8001	22.8636	1.7587
LMM-RI	-0.0407	-1.7683	0	20.6911	-0.0407
LMM-RS	-17.1775	-18.6090	-17.1438	0	-17.1775
GEE	0.0000	-1.7283	0.0407	20.7401	0

Table 5: Main effect slope percent change matrix, *MALAT1* ~ *CD19* variable pairing

Model	LM	LM-FE	LMM-RI	LMM-RS	GEE
LM	0	-5.0859	-5.5670	143.1615	0.0000
LM-FE	5.3584	0	-0.5069	156.1912	5.3584
LMM-RI	5.8952	0.5095	0	157.4964	5.8952
LMM-RS	-58.8751	-60.9666	-61.1645	0	-58.8751
GEE	0.0000	-5.0859	-5.5670	143.1615	0

Table 6: Main effect slope standard error percent change matrix, $MALAT1 \sim CD19$ variable pairing

Model	LM	LM-FE	LMM-RI	LMM-RS	GEE
LM	0	3.5197	5.8563	-50.3697	0.0000
LM-FE	-3.4000	0	2.2571	-52.0571	-3.4000
LMM-RI	-5.5323	-2.2073	0	-53.1154	-5.5323
LM-RS	101.4899	108.5816	113.2896	0	101.4899
GEE	0.0000	3.5197	5.8563	-50.3697	0

Table 7: Main effect slope test statistic percent change matrix, $MALAT1 \sim CD19$ variable pairing

Model	LM	LM-FE	LMM-RI	LMM-RS	GEE
LM	0	-83.3841	-82.8767	-78.3739	0.0000
LM-FE	501.8321	0	3.0534	30.1527	501.8321
LM-RI	484.0000	-2.9630	0	26.2963	484.0000
LM-RS	362.4047	-23.1672	-20.8211	0	362.4047
GEE	0.0000	-83.3841	-82.8767	-78.3739	0

Table 8: Main effect slope percent change matrix, $FBLN1 \sim CD34$ variable pairing

Model	LM	LM-FE	LMM-RI	LMM-RS	GEE
LM	0	-30.4878	-30.4878	48.1707	0.0000
LM-FE	43.8596	0	0.0000	113.1579	43.8596
LM-RI	43.8596	0.0000	0	113.1579	43.8596
LM-RS	-32.5103	-53.0864	-53.0864	0	-32.5103
GEE	0.0000	-30.4878	-30.4878	48.1707	0

Table 9: Main effect slope standard error percent change matrix, $FBLN1 \sim CD34$ variable pairing

Model	LM	LM-FE	LMM-RI	LMM-RS	GEE
LM	0	-4.5977	-1.2994	-41.5292	0.0000
LM-FE	4.8193	0	3.4573	-38.7114	4.8193
LM-RI	1.3165	-3.3418	0	-40.7595	1.3165
LM-RS	71.0256	63.1624	68.8034	0	71.0256
GEE	0.0000	-4.5977	-1.2994	-41.5292	0

Table 10: Main effect slope test statistic percent change matrix, $FBLN1 \sim CD34$ variable pairing

Nested Model Comparisons

Variable Pair	Model	Resid DF	RSS	DF	Sum of Squares	F-stat	P(>F)
MALAT1-CD19	LM	1108	1167.76				
	LM-FE	1094	935.89	14	231.87	19.36	6.4776e-44
FBLN1-CD34	LM	1108	650.51				
	LM-FE	1094	214.92	14	435.59	158.38	2.8058e-251

Table 11: ANOVA nested model comparison table for testing the inclusion of the subject-specific fixed-effect intercept

(Table 11) above is a nested model comparison, the result of which is an F-test statistic indicating

that there is very strong evidence to support the inclusion of the subject-specific fixed-effect intercept into the LM model.

Variable Pair	Model	df	AIC	logLik	L.Ratio	p-value
MALAT1-CD19	LM	3	3224.097	-1609.048		
	LMM-RI	4	3032.024	-1512.012	194.0722	4.1068e-44
FBLN1-CD34	LM	3	2572.807	-1283.403		
	LMM-RI	4	1438.086	-715.043	1136.72	3.4517e-249

Table 12: ANOVA nested model comparison table for testing the inclusion of the subject-specific random effect intercept

(Table 12) above is a nested model comparison, the result of which is a likelihood ratio statistic indicating that there is very strong evidence to support the inclusion of the subject-specific random effect intercept into the LM model.

Variable Pair	Model	df	AIC	logLik	L.Ratio	p-value
MALAT1-CD19	LMM-RI	4	3032.024	-1512.012		
	LMM-RS	6	2993.820	-1490.910	42.20503	6.8437e-10
FBLN1-CD34	LMM-RI	4	1438.086	-715.043		
	LMM-RS	6	1438.068	-713.034	4.018095	0.1341

Table 13: ANOVA nested model comparison table for testing the inclusion of the subject-specific random effect slope

(Table 13) above is a nested model comparison, the result of which is a likelihood ratio statistic indicating that there is very strong evidence to support the inclusion of the subject-specific random effect slope into the LMM-RI model for the $MALAT1 \sim CD19$ variable pairing. However, there is insufficient evidence to support the inclusion of the subject-specific random effect slope into the LMM-RI model for the $FBLN1 \sim CD34$ variable pairing.

Discussion

Here, I compare five modeling strategies for detecting subject level associations in single-cell RNA sequencing data gathered over 27 subjects from a Lupus Nephritis study. I compare estimates of a fixed effect slope parameter generated by five modeling techniques: linear modeling (LM), linear modeling with subjects modeled as fixed effects (LM-FE), linear mixed effects models with subjects modeled as random intercepts (LMM-RI) and random slopes (LMM-RS), and generalized estimating equations (GEE).

I find that population average models (i.e. LM and GEE) and subject specific intercept models (i.e. LMM-RI and LMM-RS) tend to produce similar results within the same model class (population average or subject specific intercept) but different results between model classes. The highest standard errors are indicated in the LMM-RS model, and the lowest standard errors in the LMM-RI model. LM-FE standard error is also found to be smaller than both LM and GEE standard error values. Nested model comparisons indicate that inclusion of subject specific terms is advisable at all levels (fixed and random, intercept and slope) with exception of the random slope in the $FBLN1 \sim CD34$ variable paring.

Interpretations of subject specific parameters are contextually authentic provided that they are used in inference conditional to their subject of origin. Conversely, interpretations of population average parameters are accurate when they are used for inference on a population’s hypothetical representation of centrality. Under conditions of linearity and error normality, it can be shown that subject specific parameters are marginal representations of population average parameters. This distinction explains the parameter estimate disparities as estimated between the LM/GEE methods compared to the LM-FE/LMM-RI methods.

This analysis is subject to several drawbacks and limitations. All the results are based on evidence obtained from just two single-cell RNA sequencing variable pairings. In the future, comparing the consistency of these models over all model pairs is needed. Additionally, single-cell RNA sequencing data is heavily influenced by protocol dependencies and measurement inconsistencies. Quality control must be carefully considered and conducted prior to any analysis.

The utility and promise of single-cell RNA sequencing data indicates that such data will become more prevalent and will be extended to multiple subject samples. I have presented an initial comparison of methods for detecting subject-level associations in single-cell RNA sequencing data sets.

Appendix

A: Data Quality Control

I use the Seurat Guided Clustering Tutorial [9] to perform quality control (QC) of the initial data. This process quantifies the quality of each single-cell observation in two numerical measures (based upon two calculated variables, **nFeature** and **PerctMT**). Threshold values of these variables are chosen and used to filter cells (observations) not meeting the chosen criteria. The Seurat tutorial provides methods of automated calculation and filtering implemented by Arazi, Rao, Berthier, et al. in [3]. Identical variable calculations, with alternative threshold settings are independently implemented for this study.

The quality control variables are conceptually defined as:

1. **nFeature** is the number of unique genes detected to have a non-zero expression in each cell. This is used to identify cells with an abnormally low or high number of expressed genes. Low numbers may result from empty wells (zero content measurements) or broken (partial) cells, while high numbers may result from observations of more than one cell.
2. **PerctMT** is the percentage of reads that map to the mitochondrial genome. This is used to identify dead and/or broken cells as dead or dying cells will retain RNAs in mitochondria, but lose cytoplasmic RNA [2].

The pre-QC distribution of **PerctMT** for each subject is displayed in (**Figure 1**) below:

The QC measure thresholds employed by Arazi, Rao, Berthier, et al. in [3] are:

1. $1,000 < \mathbf{nFeature} < 5,000$
2. $\mathbf{PerctMT} \leq 25\%$

All observations for which the calculated values of **nFeature** and **PerctMT** satisfied the inequalities in (1) and (2) above were kept, and the others were considered “low-quality” and removed. The resulting distribution of the **PerctMT** variable is displayed in (**Figure 2**):

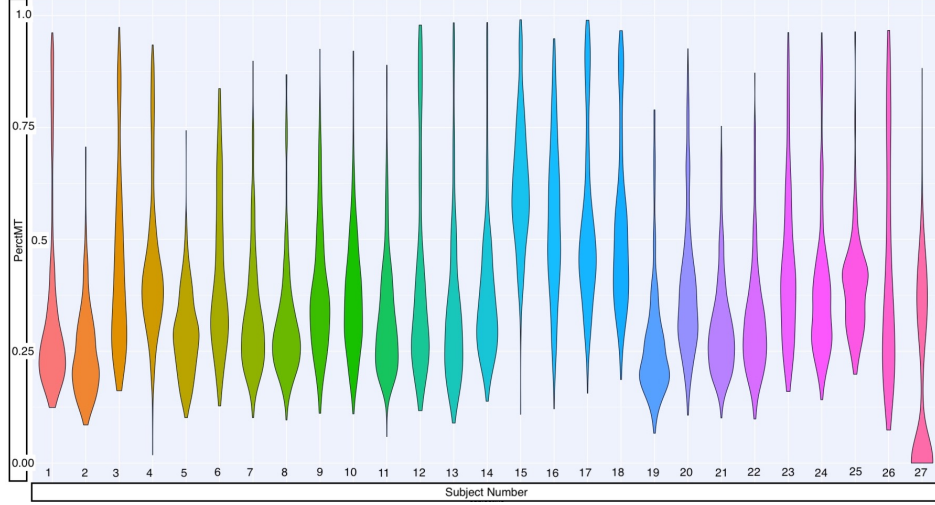


Figure 1: Pre-QC **PerctMT** Distribution for each subject

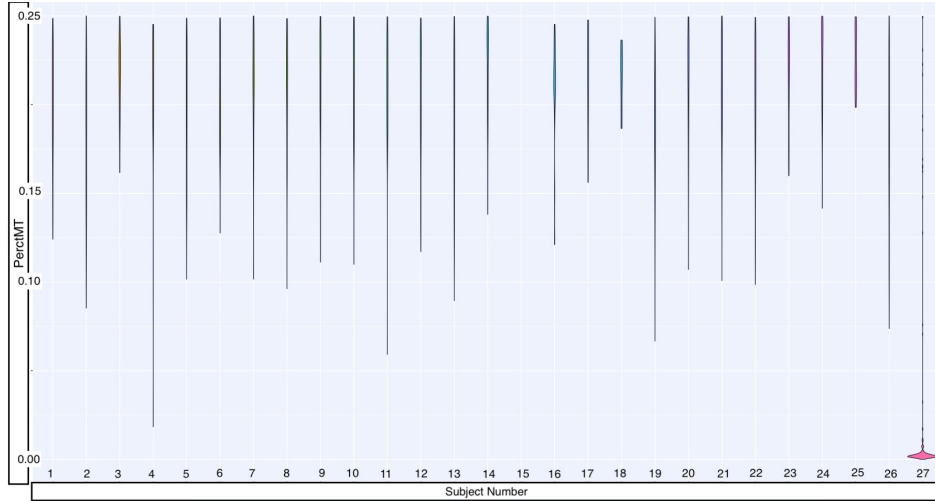


Figure 2: Post QC distribution of **PerctMT** with thresholds implemented by Arazi, Rao, Berthier, et al

As 84% of cells as removed with the filters chosen by Arazi et al, I choose a more lenient threshold, removing observations with **PerctMT** $\leq 60\%$, in an effort to keep more cells.

An additional restriction of the data to only B-cells is made in an effort to regularize the data sample (i.e. homogenize feature expression). The resulting distribution of **PerctMT** is displayed in (**Figure 3**) after filtering.

The distribution of observations for each subject Pre/Post QC (with updated **PerctMT** $\leq 60\%$ threshold value) is shown numerically in (**Table 1**):

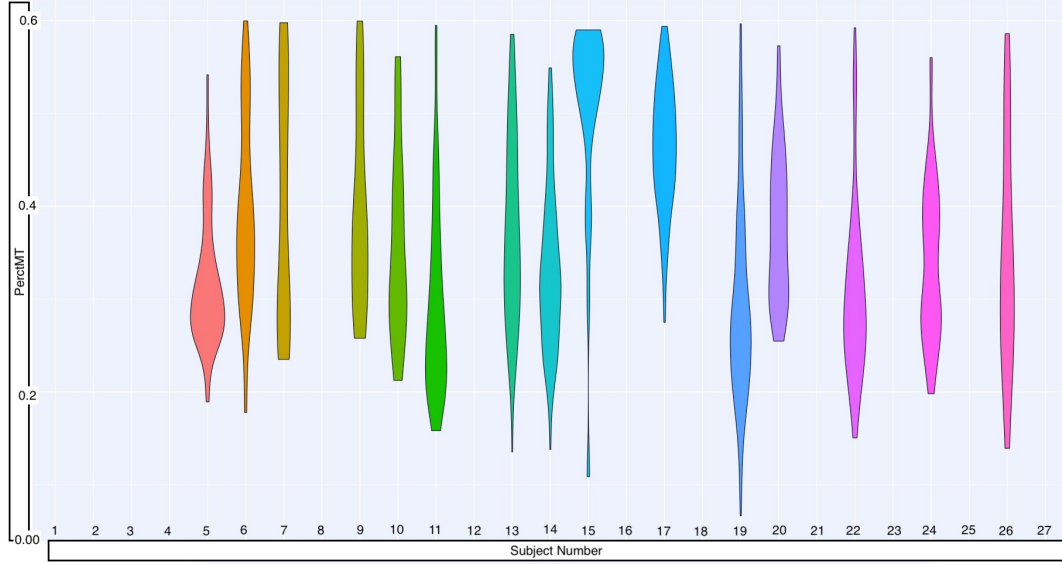


Figure 3: Post QC distribution of **PerctMT** with thresholds implemented in this paper

Subject Number	1	2	3	4	5	6	7	8	9
NO of Obs Before QC	375	375	364	381	340	383	383	356	372
NO of Obs After QC	0	0	0	0	58	86	32	0	31
Subject Number	10	11	12	13	14	15	16	17	18
NO of Obs Before QC	327	311	379	375	345	371	381	381	377
NO of Obs After QC	21	107	0	107	100	25	0	122	0
Subject Number	19	20	21	22	23	24	25	26	27
NO of Obs Before QC	380	381	380	333	333	239	218	378	342
NO of Obs After QC	127	75	0	87	0	79	0	53	0

Table 1: Observation counts per-subject Pre/Post QC with updated **PerctMT** $\leq 60\%$ threshold value.

MIN	1st Q	Median	Mean	3rd Q	MAX
21	42.5	79	74.0	103.5	127

Table 2: observation count per-subject summary statistics Post QC with updated **PerctMT** $\leq 60\%$ threshold value

B: Variable Selection and Summaries

I select two pairs of variables from the 38,354 genetic markers in the Lupus Data to compare across the five modeling methods. The variables I choose have higher values of correlation than arbitrary variable pairings as indicated by a high Pearson Correlation Coefficient (both selected pairings are within the top 10% of highest Pearson Correlation Coefficients of all possible pairings), and have previously been associated with human diseases or conditions (e.g. cancer treatment research in the case of MALAT1 [6]-used as the first outcome, or observed limb malformations in the case of FBLN1 [7]-used as the second outcome). I also attempt to assign predictor-pairings of interest. The CD19 marker (the predictor paired with MALAT1) is a transmembrane protein encoded by the CD19 gene. The FlowJo cytometry measurements contain CD19 protein readings, so the relationship between CD19 as a predictor and the outcome of interest (MALAT1) can be modeled using proteomic or transcriptomics data. CD34, the predictor which I link with FBLN1 is also a transmembrane protein encoded by a gene, and similarly interesting.

Without undergoing the process of expression normalization, single-cell RNA sequencing data is represented as non-negative integer count values. Higher counts correspond to higher detection frequencies and these detection frequencies can be interpreted as a quantification of the magnitude of expression for a transcriptomic marker (e.g CD19, CD34, MALAT1, FBLN1).

I provide numerical summaries of the four selected variables in **Tables (B1) - (B4)**. Each describes selected variable summary statistics (minimum, maximum, average, and median) for the positive observational count subjects in (**Table 1**).

Measurements of scRNA-seq data are specific to precise transcriptomic targets. This means that single-cell expression profiles (a single observation) can be limited to a small transcriptomic scope. So while the agglomerated scope of gene expression across a sample is the same as (or broader than) a traditional bulk experiment, individual observations have a biologically inflated zero-component. There are also *technical* zero-inflation components that are associated with protocol variations, and measurement error. Together, these factors contribute to right-skewed variable distributions (**Figure 4**)

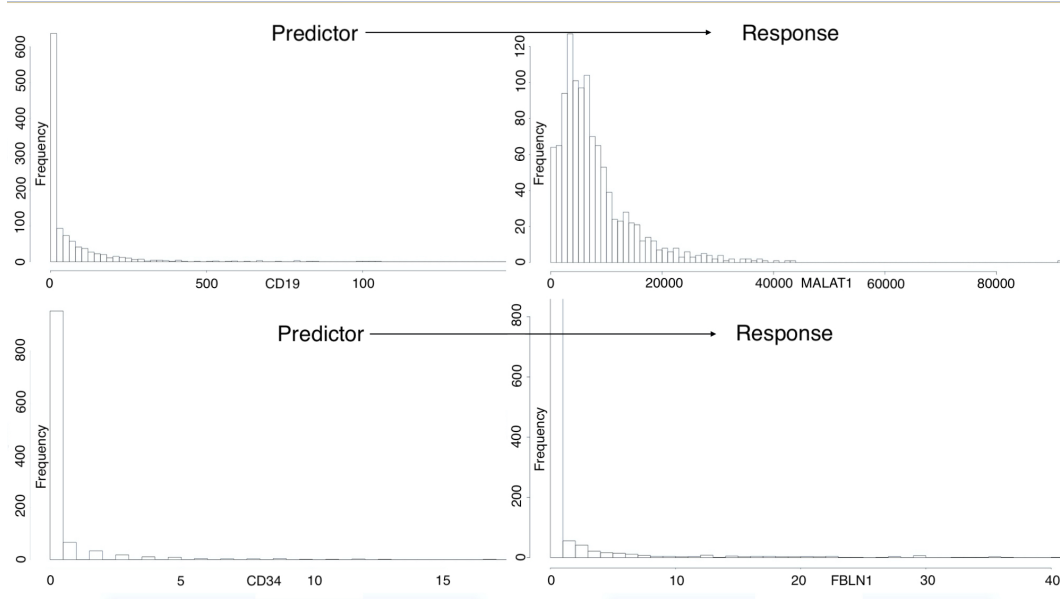


Figure 4: Predictor-Response pairing variable distributions

The MALAT1 variable has a large minimum outcome compared to the other variables, so I translate all the values of this variable *negatively* by the minimum value.

$$\min(\text{MALAT1}) = 67$$

This gives a minimum expression value of zero, which coincides with intuition as well as the minimum value of the other variables under investigation.

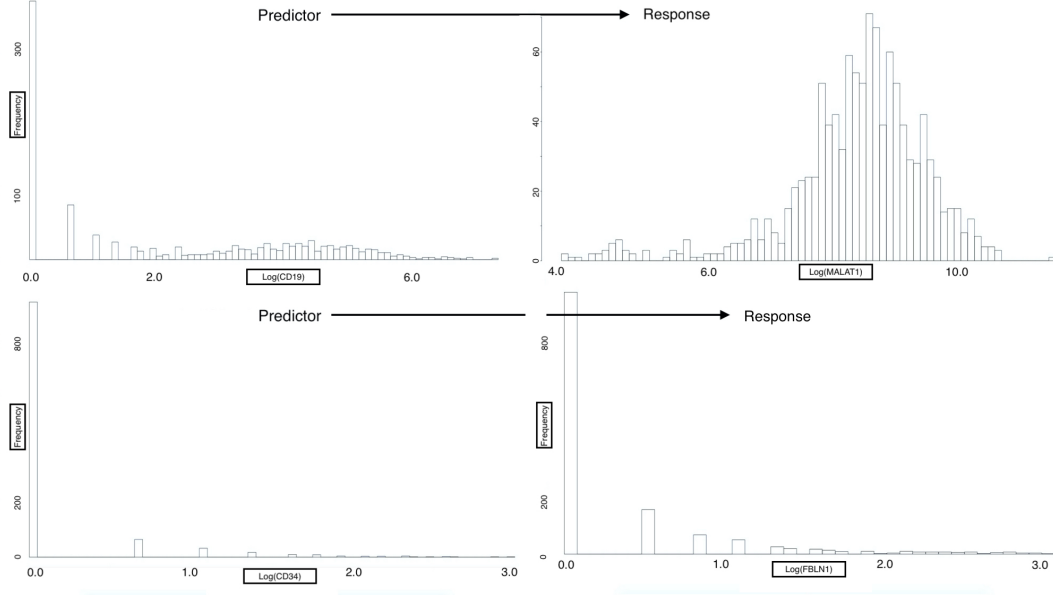
The modeling methodologies I employ motivate a log-transformation in an attempt to achieve approximate normality, especially for the outcome variable’s distribution. I perform the “log plus +1” transformation on all variables (predictor and outcome):

$$X \mapsto \log(X + 1)$$

The resulting distributions are shown in (**Figure 5**)

Figure 5: Predictor-Response variable pairings, post-transformation distributions

The log-transformed response of MALAT1 is approximately normally distributed; however, the



log-transformed response FBLN1 is not inherently better than the un-transformed response.

Regardless, each outcome is modeled under the assumption that: compensating for observational correlation will sufficiently account for non-normality of the responses. It may be the case that additional transformations and/or alternative modeling techniques may be needed to improve model error distributions. However, for the purpose of comparing the previously mentioned models on subject-correlated single-cell data, I proceed with this assumption and I verify residual homoscedasticity, normality and independence using fitted vs residual plots and quantile-quantile plots.

Table A1

CD19 Summaries

Subject Number	Minimum	Maximum	Average	Median
5	0	678	36.6724	0.0
6	0	299	36.6860	7.5
7	0	10	2.1250	1.0
9	0	1052	89.4194	3.0
10	0	158	37.5714	2.0
11	0	339	28.3178	1.0
13	0	629	56.0841	18.0
14	0	251	42.2600	19.0
15	0	148	26.6000	0.0
17	0	982	112.3770	16.0
19	0	665	59.3386	5.0
20	0	287	40.1200	23.0
22	0	380	43.4483	1.0
24	0	282	55.0127	27.0
26	0	1624	268.4151	110.0

Table A1: Predictor *CD19* variable summaries ($CD19 \sim MALAT1$)

Table A2

MALAT1 Summaries

Subject Number	Minimum	Maximum	Average	Median
5	67	40812	10206.3621	9195.0
6	757	30774	11568.2791	11689.0
7	441	17916	6868	4039.5
9	311	18239	5703.9355	5983.0
10	1875	17160	6638.5714	6190.0
11	349	34082	9716.0280	8826.0
13	99	25572	5867.9439	4895.0
14	355	15740	6154.1500	5720.5
15	157	11923	3839.0800	3467.0
17	337	8342	2960.2541	2692.0
19	227	91961	13959.9843	10125.0
20	379	21736	7301.4133	6417.0
22	161	28429	6881.7471	5068.0
24	240	42792	6248.8228	5955.0
26	1114	32426	8463.1698	6426.0

Table A2: Response *MALAT1* variable summaries (*CD19* ~ *MALAT1*)

Table A3

CD34 Summaries

Subject Number	Minimum	Maximum	Average	Median
5	0	19	3.0517	1
6	0	0	0	0
7	0	0	2	1
9	0	6	0.4516	0
10	0	5	0.6667	0
11	0	7	1.2056	1
13	0	0	0	0
14	0	1	0.4000	0
15	0	0	0	0
17	0	0	0	0
19	0	0	0	0
20	0	2	0.1867	0
22	0	4	0.3563	0
24	0	5	0.2911	0
26	0	0	0	0

Table A3: Predictor $CD34$ variable summaries ($CD34 \sim FBLN1$)

Table A4

FBLN1 Summaries

Subject Number	Minimum	Maximum	Average	Median
5	3	41	19.3448	18
6	0	0	0	0
7	0	16	4.2500	3
9	0	8	1.8710	1
10	0	30	11.9524	10
11	0	8	1.5140	1
13	0	1	0.0093	0
14	0	5	0.5700	0
15	0	1	0.0400	0
17	0	3	0.0246	0
19	0	2	0.0157	0
20	0	9	2.5867	2
22	0	11	0.9885	0
24	0	4	0.4557	0
26	0	0	0	0

Table A4:: Response *FBLN1* variable summaries ($CD34 \sim FBLN1$)

Code and Data

All code for the above analysis was written and evaluated in RStudio Version 1.2.1335, and is available for download at the following GitHub repository:

https://github.com/leepanter/MSproject_RBC.git

Additionally, a link to all necessary and reference data files (including original data) are contained in the following Google Drive:

https://drive.google.com/open?id=1gjHaMJG0Y_kPYWj5bIE4gRJU5z9R2Wqb

References

1. Macaulay IC, Voet T (2014) Single cell genomics: Advances and future perspectives. *PLoS genetics* 10: e1004126.
2. Bacher R, Kendzierski C (2016) Design and computational analysis of single-cell rna-sequencing experiments. *Genome biology* 17: 63.
3. Arazi A, Rao DA, Berthier CC, et al. (2018) The immune cell landscape in kidneys of lupus nephritis patients. *bioRxiv* 363051.
4. FlowJo X V10. 0.7 r2 flowjo. LLC <https://www.flowjo.com>.
5. Hashimshony T, Senderovich N, Avital G, et al. (2016) CEL-seq2: Sensitive highly-multiplexed single-cell rna-seq. *Genome biology* 17: 77.
6. Gutschner T, Hämmerle M, Diederichs S (2013) MALAT1—a paradigm for long noncoding rna function in cancer. *Journal of molecular medicine* 91: 791–801.
7. Debeer P, Schoenmakers E, Twal W, et al. (2002) The fibulin-1 gene (fbln1) is disrupted in at (12; 22) associated with a complex type of synpolydactyly. *Journal of medical genetics* 39: 98–104.
8. Fitzmaurice GM, Laird NM, Ware JH (2012) Applied longitudinal analysis, John Wiley & Sons.

9. Satija R, others (2018) Seurat: Guided clustering tutorial. *Satija Lab* http://satijalab.org/seurat/pbmc3k_tutorial.html.